http://doi.org/10.35784/iapgos.5498 *received: 23.10.2023 | revised: 18.02.2023 | accepted: 14.03.2024 | available online: 31.03.2024*

CORRESPONDENCE MATCHING IN 3D MODELS FOR 3D HAND FITTING

Maksym Tymkovych[1], Oleg Avrunin[1], Karina Selivanova[1], Alona Kolomiiets[2], Taras Bednarchyk[3], Saule Smailova[4]

[1]Kharkiv National University of Radio Electronics, Kharkiv, Ukraine, [2]Vinnytsia National Technical University, Vinnytsia, Ukraine, [3]Vinnytsia Pyrohov National Medical University, Vinnytsia, Ukraine, [4]D.Serikbayev East Kazakhstan State Technical University, Ust-Kamenogorsk, Kazakhstan

Abstract. *Upper limb prosthetic is an area of medical research and development that aims to restore functionality and improve the quality of life of people affected by the loss of one or both upper limbs. The development and implementation of 3D scanning tools and analysis of 3D scanning data requires the use of specialized analysis methods that ensure the achievement of the required indicators. It should take into account the impact of the model resolution on the result. This paper is devoted to the analysis of finding matches between a point cloud of a hand model and another point cloud using Gromov-Wasserstein distance. For analysis, a subset of the MANO dataset was employed, containing a substantial volume of data and serving as a representative sample of the human population. The results obtained indicate the possibility of using this approach in the processing and analysis of three-dimensional data, which serves as one of the stages of designing individualized prostheses.*

Keywords: health care, medical technology, physical rehabilitation, 3D modeling, correspondence matching

DOPASOWANIE ZGODNOŚCI W MODELACH 3D DLA DOPASOWANIA DŁONI 3D

Streszczenie. *Protetyka kończyn górnych to dziedzina badań i rozwoju medycznego mająca na celu przywrócenie funkcjonalności i poprawę jakości życia osób dotkniętych utratą jednej lub obu kończyn górnych. Opracowanie i wdrożenie narzędzi do skanowania 3D oraz analiza danych pochodzących ze skanowania 3D wymaga zastosowania specjalistycznych metod analizy, które zapewnią osiągnięcie wymaganych wskaźników. Należy przy tym uwzględnić wpływ rozdzielczości modelu na uzyskany wynik. Niniejszy artykuł poświęcony jest analizie znajdowania dopasowań między chmurą punktów modelu dłoni a inną chmurą punktów przy użyciu odległości Gromova-Wassersteina. Do analizy wykorzystano podzbiór zbioru danych MANO, który zawiera znaczną ilość danych i służy jako reprezentatywna próbka populacji ludzkiej. Uzyskane wyniki wskazują na możliwość wykorzystania tego podejścia w przetwarzaniu i analizie danych trójwymiarowych, które służą jako jeden z etapów projektowania zindywidualizowanych protez*.

Słowa kluczowe: opieka zdrowotna, technologia medyczna, rehabilitacja fizyczna, modelowanie 3D, dopasowanie

Introduction

The wide-scale aggression against Ukraine has resulted in injuries to a significant number of individuals across different age groups, professions, and social statuses. This has already led to a shortage of appropriate resources in both the domestic and international markets. The development of accessible and cost-effective solutions enabling the modeling, simulation, fabrication, and testing of prosthetic devices for a wide audience is essential. In this context, the mathematical foundations, theoretical advancements, and practical research must be presented to facilitate their implementation. It should be noted that in the case of prosthetics for children, the prosthetic process usually involves multiple stages due to the healthy growth of children, necessitating prosthetic updates [1, 7, 9].

Furthermore, the market demands not only a certain quantity of specialized materials and products but also specialized devices (such as scanners) that enable the scanning and digitization of the hand, thereby facilitating the personalization of the prosthesis [8, 20]. Moreover, in the current landscape, a multitude of scanners exists, encompassing diverse pricing tiers and being founded upon various underlying technologies. Notably, scanners employing techniques such as photogrammetry, Time of Flight, and others emerge, each imbued with its unique capabilities [6, 14, 16]. These advancements facilitate precise measurements and digitization of anatomical structures, thereby fostering the development of highly customized and tailored prosthetic solutions. The availability of a wide spectrum of scanning technologies empowers researchers and practitioners alike to select the most suitable and effective approach for capturing intricate anatomical details. Photogrammetry, for instance, leverages the principles of triangulation from multiple images, enabling accurate three-dimensional reconstructions [9]. On the other hand, Time of Flight scanners utilize the measurement of light travel time to create detailed depth maps, ensuring high precision [5, 27]. Such technological diversity is a testament to the rapid progress in the field, opening doors for innovative solutions and personalized prosthetic designs.

However, measurements based on the polygonal model data require monotonous work from operators, which is not always convenient. Moreover, contemporary medical solution development practices focus on automating both the analysis and the automatic modeling (with varying degrees of interaction), offering numerous advantages [2, 11, 12]. Thus, there is a need for scientific research to address these challenges and explore the benefits of automating the analysis [21, 22, 24] and modeling processes in the field of prosthetics for efficient and personalized solutions [18, 22, 26].

In the realm of polygonal model analysis, a crucial undertaking revolves around the delineation of anatomical landmarks – distinctive elements corresponding to specific anatomical structures. In the context of the human upper limb, fingers stand out as prominent and recognizable landmarks. Consequently, the simplest constituent of a polygonal model manifests as the distal segment of a finger, which aptly encapsulates the digit's 'culmination.' Thus, the fundamental objective entails establishing correlations among the five anatomical markers of a reference model – representing the fingers' extremities – and the corresponding five markers within a target model. It is noteworthy to highlight that a principal challenge stems from the irregularity inherent in the input structure, coupled with the absence of a well-defined regular grid-like pattern. This intricacy substantially complicates the applicability of solutions rooted in Convolutional Neural Networks (CNNs). The irregular and often unstructured nature of anatomical models poses a unique hurdle, necessitating innovative approaches that transcend the conventional paradigms of neural network utilization. This foundational alignment not only serves as a cornerstone for subsequent analyses but also paves the way for a myriad of insights. Such alignments facilitate advanced examinations, spanning the segmentation of complete fingers, delineation of distinct anatomical segments, and extraction of specific anatomical characteristics. Consequently, the primary thrust of this work materialized as an exploration of methodologies to uncover correspondences between digitized hand models, coupled with a rigorous assessment of their efficacy.

By embarking on this journey, we aim to harness the potential of these correspondences as a potent tool for various applications, ranging from personalized prosthetic design to ergonomic studies and beyond. Through a comprehensive exploration of these inter-model relationships, we endeavor to unlock novel avenues for enhancing the precision, utility, and impact of anatomical modeling in both research and practical applications [10, 13, 25].

1. Materials and methods

The foundation of this study was established using the MANO dataset [15], comprising three-dimensional polygonal hand models, as depicted in figure 1.

a b c d

Fig. 1. Visualization of initial hand scans in the zero position: a) models "on top of each other", b) 01_01r.ply, c) 06_01r.ply, d) 09_01r.ply

Specifically selected for this investigation, the dataset features a diverse range of hand scans, encompassing various poses. Furthermore, it is pertinent to note that exclusively scans of the right hand were employed in this study. This deliberate selection serves to streamline the complexity of the task by focusing on a singular hand configuration, enhancing the interpretability of results and facilitating a more targeted analysis For the initial phase of research, data corresponding to an open-palm pose were utilized, effectively considered as the 'neutral' position. Moreover, a subset of the 3D models was chosen, as outlined in table 1.

Each polygonal model underwent a simplification process, transforming them into point clouds while preserving key metrics, as detailed in table 2. MeshLab [3] was employed for this simplification procedure, utilizing the Quadric Collapse Edge Decimation function [4]. This technique facilitates the reduction of computational complexity by intelligently collapsing edges, resulting in streamlined point cloud structures.

Consequently, the resultant three-dimensional point clouds (Fig. 2) exhibited the quantifiable attributes outlined in table 2. These parameters serve to expedite calculations, enabling quicker processing times and the judicious utilization of system memory resources. This streamlined data representation proves essential for the subsequent algorithmic phases, enhancing computational efficiency and scalability while laying the groundwork for more advanced analyses.

Additionally, each such model underwent further annotation, encompassing the identification of vertices corresponding to the distal segment of each finger, essentially the fingertip. In this process, due consideration was given to the inherent variability within the dataset, accounting for nuances and potential ambiguities. Notably, the annotation process revealed a nuanced characteristic: the correspondence between specific finger tips and vertices is not always a one-to-one relationship, but rather a discernible grouping.

a b c d

Fig. 2. Visualization of optimized hand point clouds in the zero position: a) models "on top of each other", b) 01_01r.ply, c) 06_01r.ply, d) 09_01r.ply

Table 1. Quantitative indicators of the initial dataset

File Name	Vertices count	Faces count	File Name	Vertices count	Faces count
01_01r.ply	39003	77592	34_01r.ply	42745	85083
06_01r.ply	37398	74338	35_01r.ply	36082	71574
09_01r.ply	48553	96714	36_01r.ply	43123	85771
15_01r.ply	43919	87393	39_01r.ply	43456	86501
18_01r.ply	49572	98530	40_01r.ply	51491	102430
27_01r.ply	36166	72027	41_01r.ply	32189	64069
30_01r.ply	39955	79447	43_01r.ply	45013	89534
32_01r.ply	43597	86500	50_01r.ply	41846	83340

Table 2. Quantitative indicators of processed point clouds

File Name	Vertices count	File Name	Vertices count	File Name	Vertices count
01_01r.ply	2019	30_01r.ply	2014	40_01r.ply	2020
06_01r.ply	2018	32_01r.ply	2021	41_01r.ply	2019
09_01r.ply	2018	34_01r.ply	2028	43_01r.ply	2018
15_01r.ply	2017	35_01r.ply	2025	50_01r.ply	2021
18_01r.ply	2019	36_01r.ply	2018		
27_01r.ply	2018	39_01r.ply	2020		

Furthermore, in tandem with vertex selection, the annotation also involved a subjective assignment of radii, delineating the region associated with the fingertip. This iterative and subjective process aimed to capture the spatial extent accurately. This meticulous annotation methodology yielded the dataset detailed in Table 3, encapsulating the crucial spatial attributes of the distal finger segments across the selected models.

Figure 3 illustrates two plots: the distribution of radii for each of the fingers, as well as the vertex count distribution for each of the fingers.

An instance of annotated distal fingertip regions from a specific subset of the right-hand dataset is presented in figure 4.

As evident from the illustrations, the hand coordinate systems exist in diverse planes and lack a shared orientation. Hand dimensions, finger orientations, and deformations exhibit non-uniform variations. Consequently, the task of aligning corresponding markers between one point cloud and another is inherently intricate.

Table 3. Annotated fingertip data

File Name	Thumb Vertex Count	Thumb Radius, (Rel. Units)	Index Vertex Count	Index Radius, (Rel. Units)	Middle Vertex Count	Middle Radius, (Rel. Units)	Ring Vertex Count	Ring Radius, (Rel. Units)	Little Vertex Count	Little Radius, (Rel. Units)
01_01r.ply	11	0.006533	5	0.004197	7	0.005311	8	0.005311	4	0.00344
09_01r.ply	12	0.007458	13	0.007417	12	0.007417	7	0.005268	12	0.005398
39_01r.ply	17	0.007024	8	0.005022	9	0.006026	9	0.006886	9	0.00506
27_01r.ply	18	0.007211	18	0.007293	10	0.006537	13	0.006179	6	0.004006
43_01r.ply	15	0.007978	10	0.006492	8	0.005536	9	0.006407	5	0.005263
40_01r.ply	13	0.007393	13	0.007139	8	0.006091	8	0.006153	13	0.004701
50_01r.ply	13	0.006932	8	0.004814	9	0.005315	11	0.005976	12	0.006107
36_01r.ply	19	0.007367	12	0.007282	12	0.006313	5	0.004762	6	0.004587
30_01r.ply	20	0.006142	21	0.007532	12	0.006327	12	0.005476	7	0.004163
18_01r.ply	23	0.007729	8	0.005478	7	0.005707	9	0.006218	8	0.005185
35_01r.ply	16	0.007708	15	0.007209	10	0.005076	21	0.007485	6	0.004445
32_01r.ply	15	0.006418	14	0.007742	8	0.00537	7	0.005344	6	0.005175
41_01r.ply	12	0.005582	16	0.006202	13	0.006425	12	0.005168	8	0.003938
06_01r.ply	18	0.00699	12	0.006861	11	0.005738	10	0.005358	8	0.004345
15_01r.ply	32	0.008502	12	0.006458	9	0.006162	9	0.00611	6	0.004455
34_01r.ply	27	0.008376	14	0.007543	13	0.007705	8	0.005127	3	0.004349

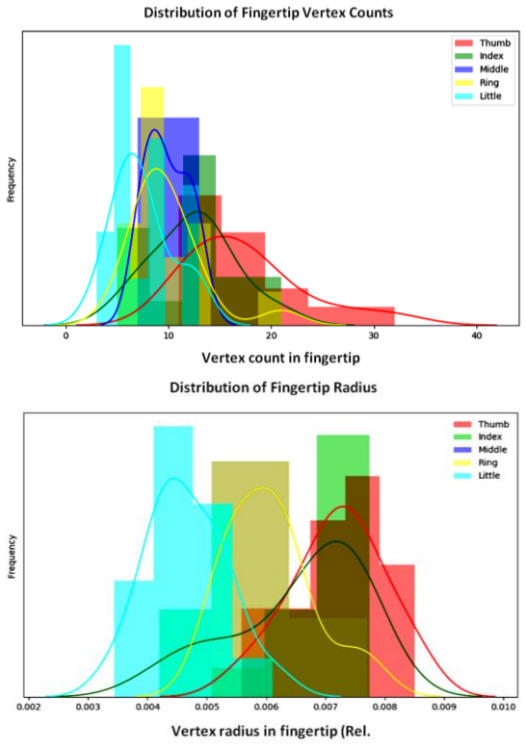

Fig. 3. Comparison of Fingertip Radius and Vertex Distribution

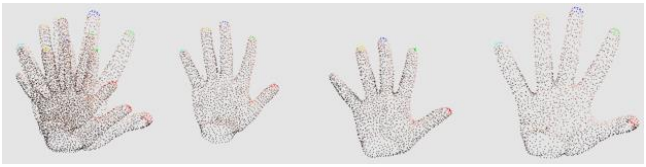

a b c d

Fig. 4. Example of annotated point clouds of a 3D hand model: a) models "on top of each other", b) 01_01r.ply, c) 06_01r.ply, d) 09_01r.ply

Thus, the fundamental 3D hand model can be generalized as a point cloud representation ($X_1 \in \mathbb{R}^3$):

$$X_1 = \{(x_{11}, y_{11}, z_{11}), (x_{12}, y_{12}, z_{12}), ..., (x_{1m}, y_{1m}, z_{1m})\} \quad (1)$$

where x_{11}, y_{11}, z_{11}, x_{1m}, y_{1m}, x_{1m} are coordinates of corresponding point of point cloud.

Similarly, the target 3D hand model is described by a point cloud representation ($X_2 \in \mathbb{R}^3$):

$$X_2 = \{(x_{21}, y_{21}, z_{21}), (x_{22}, y_{22}, z_{22}), ..., (x_{2m}, y_{2m}, z_{2m})\} \quad (2)$$

For each finger tip i, let A_{1i}, and A_{2j} be anatomical landmarks represented as subsets of points in their respective point clouds.

$$A_{1i}, X_1, \text{ for } i = 1, 2, ..., 5 \quad (3)$$

and:

$$A_{2j}, X_2, \text{ for } j = 1, 2, ..., 5 \quad (4)$$

The goal is to find a mapping function $f : A_{1}i \rightarrow A_{2}j$, where f establishes correspondence between anatomical landmarks:

$$f: A_{1i} \rightarrow A_{2j}, \text{ for } j \in \{2, 3, 4, 5\} \quad (5)$$

Moreover, it should be noted that to evaluate the performance of the function *f*, a quality assessment criterion must be chosen. Given the substantial complexity of such a function and its inherent ambiguity, we will employ the following loss function:

$$Loss_{logic}(A_{1i},B_{1ik})=[A_{1i} \cap B_{1ik} \neq \emptyset] \quad (6)$$

where A_{1i} is the set corresponding to annotated ground-truth data for anatomical area *i*, B_{1ik} is the predicted set for area *i* using the mapping function *f* from point cloud *k*.

Furthermore, we will utilize the Intersection over Union (IoU) evaluation criterion (7), which quantifies the extent of vertex overlap between two sets:

$$Loss_{IoU}(A_{1i},B_{1ik})=A \cap B \,/\, A \cup B \quad (7)$$

As a function for finding the "closest" vertex from one point cloud to another, we will employ the Gromov-Wasserstein distance over distance matrices obtained from these point clouds [4, 13]:

$$GW(P,Q)=\inf_{\pi \in \Pi(X,Y)} \sum_{(x,y) \in X \times Y} c(x,y)\pi(x,y) \quad (8)$$

where *GW(P,Q)* represents the Gromov-Wasserstein distance between distributions *P* and *Q*; *X,Y* are spaces on which the distributions *P* and *Q* defined; *Π(X,Y)* is the set of all possible transport plans between distributions *P* and *Q*; *c(x,y)* is the metric or distance between objects *x* and *y*; π(x,y) is an element of the transport plan indicating how much mass is transported from object *x* to object *y*.

2. Results and discussion

Thus, for each annotated set of vertexes in the point cloud, a search for correspondences was performed on another point cloud, resulting in corresponding $Loss_{IoU}$ metrics for each finger tip (Fig. 5).

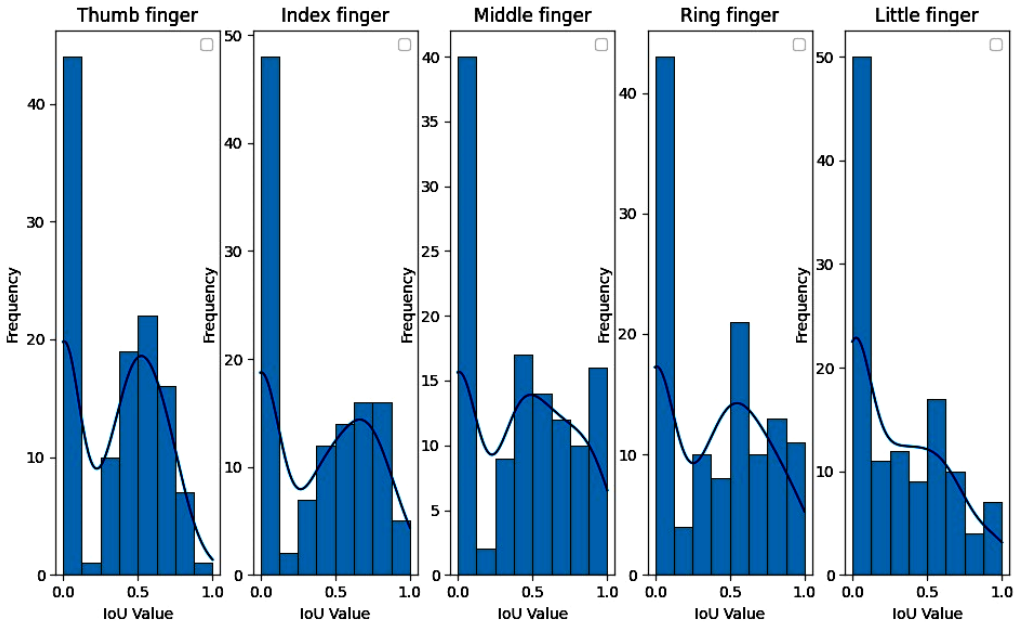

Fig. 5. Visualization of Loss IoU distribution for different fingers

The graph indicates that achieving a 100% match of annotated points is not feasible, although we consider a match of at least one vertex from the set to be sufficient. The number of matches can be increased by enlarging the radius of annotations, although this may not always be acceptable. Additionally, the distributions for all fingers appear similar, implying a consistent error pattern in both erroneously and correctly annotated sets.

An example of annotated sets of anatomical landmarks for fingertips, along with the corresponding sets obtained using equation (8), is illustrated in Fig. 6.

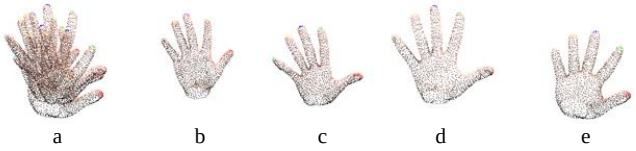

Fig. 6. Visualization of accurate matches in 3D Hand Model Point Clouds: a) models "on top of each other", b) ground truth 01_01r.ply, c) predicted 06_01r.ply from 01_01r.ply, d) 09_01r.ply predicted from 01_01r.ply, e) 15_01r.ply predicted from 01_01r.ply

As evident from the figure, the annotations correspond to anatomical landmarks, indicating the viability of the proposed approach in automating the search for anatomical landmarks. Additionally, the high level of stability of this approach is indicated by quantitative metrics, namely the $Loss_{logic}$, which is presented in the form of a diagram in Fig. 7.

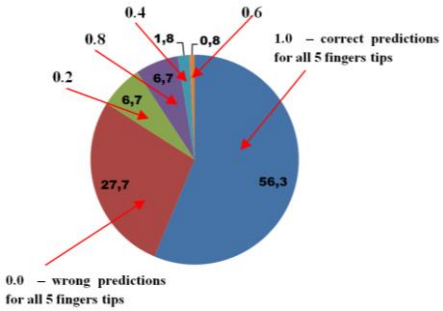

Fig. 7. Visualization of distribution of $Loss_{logic}$ in the test dataset

It should be noted that there exists a certain percentage of "inaccuracies" in the predictions. Such a level of errors can be considered acceptable for the initial stage of research and development. Furthermore, a certain level of errors is attributed to the low point cloud density and small annotation radius.

Furthermore, as evident from Fig. 8, these inaccuracies are partly attributed to the presence of certain "noisy elements" in the data, indicating the potential utilization of this method during pre-processing.

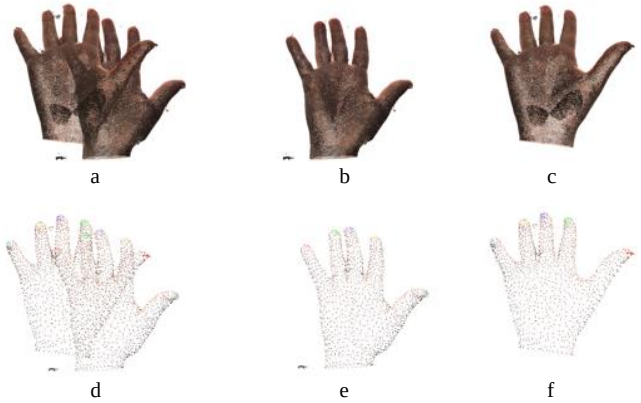

Fig. 8. Visualization of inaccurate matches in 3D Hand Model Point Clouds: a) original models "on top of each other", b) original reference model 34_01r.ply with "noise island", c) original target model 30_01r.ply, d) annotated models "on top of each other", e) ground truth annotation of reference model 34_01r.ply, f) inaccurate annotation prediction for model 30_01r.ply

3. Conclusions

The conducted research has thoroughly examined the quantitative indicators pertaining to the potential utilization of the Gromov-Wasserstein distance function for the determination of corresponding segments within a model (point clouds). These indicators attest to the promising nature of the method for applications in the development of automated prosthetic modeling tools. Furthermore, it is essential for future investigations to explore the impact of point cloud density as well as the variability in hand poses. Many patients are unable to maintain their hand in a specific pose due to various injuries, necessitating a matching function for anatomical markers that remains effective irrespective of the chosen hand pose. Such approaches can be used for image processing in a variety of medical applications, including disaster medicine and microscopic image analysis [19, 23]. The prospects of this work encompass the practical implementation of the developed method in the realm of modeling and designing personalized prosthetic devices. As such, this method holds potential to significantly enhance the accuracy and efficiency of prosthetic modeling processes, thus contributing to improved patient care and rehabilitation outcomes.

References

[1] Avrunin O. G. et al.: Application of 3D printing technologies in building patient-specific training systems for computing planning in rhinology. Proceedings of the International Scientific Internet Conference on Computer Graphics and Image Processing and 48th International Scientific and Practical Conference on Application of Lasers in Medicine and Biology, 2019, 1 [https://doi.org/10.1201/9780429057618-1].

[2] Boleneus G. J. et al.: Top-down design enables flexible design of prosthetic forearms and hands. ASEE Annual Conference and Exposition, Conference Proceedings, 2019.

[3] Cignoni P. et al.: MeshLab: an Open-Source Mesh Processing Tool. Sixth Eurographics Italian Chapter Conference, 2008, 129–136.

[4] Garland M., Heckbert P. S.: Simplifying surfaces with color and texture using quadric error metrics. Proceedings Visualization 98, 2000.

[5] Guidi G., Gonizzi S., Micoli L.: 3D capturing performances of low-cost range sensors for mass-market applications. International Archives of the Photogrammetry, Remote Sensing and Spatial Information Sciences 41, 2016, 33–40 [https:// doi.org/10.5194/isprsarchives-XLI-B5-33-2016].

[6] Kim Y. et al.: Dynamic elasticity measurement for prosthetic socket design. International Conference on Rehabilitation Robotics – ICORR, London, UK, 2017, 1281–1286 [https://doi.org/10.1109/ICORR.2017.8009425].

[7] Neri P. et al.: Semi-automatic Point Clouds Registration for Upper Limb Anatomy. International Joint Conference on Mechanics, Design Engineering and Advanced Manufacturing – JCM, 2023, 733–742 [https://doi.org/10.1007/978-3-031-15928-2_64].

[8] Neri P. et al.: 3D scanning of Upper Limb anatomy by a depth-camera-based system. International Journal on Interactive Design and Manufacturing, 2023 [https://10.1007/s12008-023-01248-1].

[9] Olsen J. et al.: 3D-Printing and Upper-Limb Prosthetic Sockets: Promises and Pitfalls. IEEE Transactions on Neural Systems and Rehabilitation Engineering 29, 2021, 527–535 [https://doi.org/10.1109/tnsre.2021.3057984].

[10] Pavlov S. V. et al.: Photoplethysmohrafic technologies of the cardiovascular control. Universum-Vinnitsa, Vinnitsa, 2007.

[11] Pavlov S. V. et al.: A simulation model of distribution of optical radiation in biological tissues. Visnyk VNTU 3, 2011, 191–195.

[12] Pavlov S. V. et al.: Laser photoplethysmography in integrated evaluation of collateral circulation of lower extremities. Proc. SPIE 8698, 2012, 869808.

[13] Peyré G., Cuturi M., Solomon J.: Gromov-Wasserstein averaging of kernel and distance matrices. International Conference on Machine Learning (ICML), 2016.

[14] Román-Casares A. M., García-Gómez O., Guerado E.: Prosthetic Limb Design and Function: Latest Innovations and Functional Results. Current Trauma Reports 4(4), 2018, 256–262 [https://doi.org/10.1007/s40719-018-0150-2].

[15] Romero J., Tzionas D., Black M. J.: Embodied hands: Modeling and capturing hands and bodies together. ACM Transactions on Graphics 36(6), 2017, 245 [https://doi.org/10.1145/3130800.3130883].

[16] Ryniewicz A. et al.: The use of laser scanning in the procedures replacing lower limbs with prosthesis. Measurement 112, 2017, 9–15.

[17] Selivanova K. G. et al.: 3D visualization of human body internal structures surface during stereo-endoscopic operations using computer vision techniques. Przeglad Elektrotechniczny 9, 2021, 30–33 [https://doi.org/10.15199/48.2021.09.06].

[18] Serkova V. et al.: Medical expert system for assessment of coronary heart disease destabilization based on the analysis of the level of soluble vascular adhesion molecules. Proc. SPIE 10445, 2017, 104453O.

[19] Sokol Y. et al.: Using medical imaging in disaster medicine. Proceedings of IEEE 4th International Conference on Intelligent Energy and Power Systems – IEPS 2020, 287–290 [https://doi.org/10.1109/IEPS51250.2020.9263175].

[20] Tymkovych M. et al.: Ice crystals microscopic images segmentation based on active contours. 2019 IEEE 39th International Conference

on Electronics and Nanotechnology – ELNANO 2019, 493–496 [https://doi.org/10.1109/ELNANO.2019.8783332].
[21] Tymkovych M. et al.: Detection of Chest Deviation During Breathing Using a Depth Camera. Proceedings of IEEE 8th International Conference on Problems of Infocommunications, Science and Technology – PIC S and T, 85 [https://doi.org/10.1109/PICST54195.2021.9772111].
[22] Tymkovych M. et al.: Application of SOFA Framework for Physics-Based Simulation of Deformable Human Anatomy of Nasal Cavity. Proceedings of IFMBE, 2021, 112 [https://doi.org/10.1007/978-3-030-64610-3_14].
[23] Tymkovych M. et al.: Application of Artificial Neural Networks for Analysis of Ice Recrystallization Process for Cryopreservation. Proceedings of IFMBE, 2021, 102 [https://doi.org/10.1007/978-3-030-64610-3_13].
[24] Wojcik W. et al.: ECTL application for carbon monoxide measurements. Proc. of SPIE 5958, 2005, 595837.
[25] Xu H. et al.: Gromov-wasserstein learning for graph matching and node embedding. International Conference on Machine Learning – ICML, 2019.
[26] Zabolotna N. et al.: Diagnostic efficiency of Mueller-matrix polarization reconstruction system of the phase structure of liver tissue, Proc. SPIE 9816, 2015, 98161E [https://doi.org/10.1117/12.2229018].
[27] Zanuttigh P. et al.: Time-of-Flight and Structured Light Depth Cameras Technology and Applications. Springer, 2016.

Ph.D. Maksym Tymkovych
e-mail: maksym.tymkovych@nure.ua

Ph.D., senior lecturer of the Department of Biomedical Engineering, Kharkiv National University of Radio Electronics, Ukraine.
Research interests: 3D visualization, biomedical image analysis, medical robotics, deep learning, artificial intelligence, computer-assisted surgery.

https://orcid.org/0000-0001-5613-1104

Prof. Oleg Avrunin
e-mail: oleh.avrunin@nure.ua

Doctor of Technical Sciences, professor, Head of Biomedical Engineering Department, Kharkiv National University of Radio Electronics, Ukraine. Scientific supervisor of research work on research of theoretical and technical principles of diagnostics, assessment and correction of medical and social human conditions. Invited Professor in Gottfried Wilhelm Leibniz Universität Hannover (Germany) and Harbin Engineering University (China).

https://orcid.org/0000-0002-6312-687X

Ph.D. Karina Selivanova
e-mail: karina.selivanova@nure.ua

Ph.D., associate professor of the Department of Biomedical Engineering, Kharkiv National University of Radio Electronics, Ukraine.
Research interests: methods of automated processing and analysis of biomedical data, study of individual characteristics of fine motor skills of hands and psychomotor skills, development of tests, complexes for psychoneurology, virtual simulators. Have more than 60 scientific publications and 1 patent of Ukraine. Participation in the international project DAAD No. 54364768 (2013), (Hannover, Germany).

https://orcid.org/0000-0003-1002-0761

D.Sc. Alona Kolomiiets
e-mail: alona.kolomiets.vnt@gmail.com

Doctor of Pedagogical Sciences, associate professor, professor of Department of Higher Mathematics, Vinnytsia National Technical University.
Research interests: professional pedagogy, the fundamentalization of the mathematical training of future bachelors of technical specialties, mathematical modeling, methods of statistical analysis of experimental data.

http://orcid.org/0000-0002-7665-6247

Ph.D. Taras Bednarchyk
e-mail: taras2010.2017@gmail.com

Vinnytsia Pyrohov National Medical University, Ph.D. (Philosophy), associate professor.
Research interest: medical ethics, bioethics, philosophy of science, methodology of scientific research, social psychology.

https://orcid.org/0000-0003-2336-4635

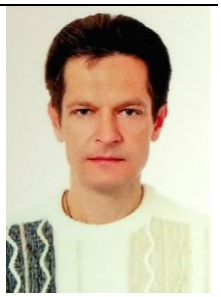

Ph.D. Saule Smailova
e-mail: Saule_Smailova@mail.ru

Saule Smailova is currently a lecturer at the School of Digital Technologies and Artificial Intelligence D.Serikbayev East Kazakhstan University, Ust-Kamenogorsk, Kazakhstan. She is a co-author over 60 papers in journals, book chapters, and conference proceedings. Member of Expert Group in the Computer Science specialization of IQAA.
Her professional interests are teaching, artificial intelligence, software engineering, data processing.

https://orcid.org/0000-0002-8411-3584